

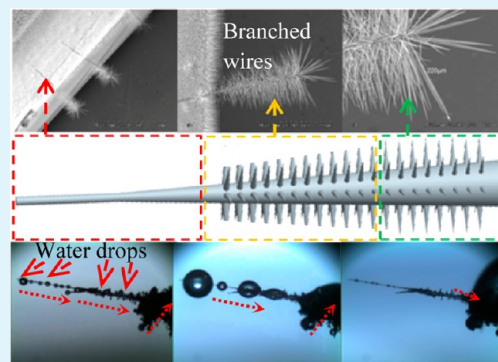
Branched ZnO Wire Structures for Water Collection Inspired by Cacti

Xin Heng,[†] Mingming Xiang,[†] Zhihui Lu, and Cheng Luo^{*}

Department of Mechanical and Aerospace Engineering, University of Texas at Arlington 500 W. First Street, Woolf Hall 226, Arlington, Texas 76019, United States

ABSTRACT: In this work, motivated by an approach used in a cactus to collect fog, we have developed an artificial water-collection structure. This structure includes a large ZnO wire and an array of small ZnO wires that are branched on the large wire. All these wires have conical shapes, whose diameters gradually increase from the tip to the root of a wire. Accordingly, a water drop that is condensed on the tip of each wire is driven to the root by a capillary force induced by this diameter gradient. The lengths of stem and branched wires in the synthesized structures are in the orders of 1 mm and 100 μm , respectively. These dimensions are, respectively, comparable to and larger than their counterparts in the case of a cactus. Two groups of tests were conducted at relative humidity of 100% to compare the amounts of water collected by artificial and cactus structures within specific time durations of 2 and 35 s, respectively. The amount of water collected by either type of structures was in the order of 0.01 μL . However, on average, what has been collected by the artificial structures was 1.4–5.0 times more than that harvested by the cactus ones. We further examined the mechanism that a cactus used to absorb a collected water drop into its stem. On the basis of the gained understanding, we developed a setup to successfully collect about 6 μL of water within 30 min.

KEYWORDS: cactus, fog, dew, water collection, branched ZnO wire structures, conical wires



1. INTRODUCTION

Deserts roughly cover about one-quarter of the Earth's land area, and semideserts another quarter.¹ They have little rainfall every year. Fog and dew in some deserts may deliver more water than rainfall,¹ and may be important water sources, e.g., to beetles, cacti, dune grasses, and *cotula fallax* plants.^{2–5} What these species use to collect water from fog and dew in a desert obviously provides a new insight to obtain water. It is particularly important to residents living in an arid environment, since fog and dew may always exist when temperature is decreased in late nights and early mornings.

It is reported that a beetle living in the Namib Desert can collect water from fog and dew through microbumps on its back. The peaks of these microbumps are hydrophilic, whereas the troughs are superhydrophobic.² The water in the fog forms fast-growing drops on these peaks. As a drop reaches a size of 4 to 5 mm in diameter, the drop overcomes the capillary force that makes it attach to the peak, and rolls down the beetle's surface to the mouthpart.² It is also reported that the cactus *O. microdasys*, originated from the Chihuahua Desert, can also harvest water from the fog and dew using the spines distributed on its surface.³ Microbarbs are grown on a spine, forming a branched wire structure. The spine may be visualized as the stem wire in the structure, whereas the relatively small microbarbs may be considered as branched wires. The spine and microbarb have lengths with the orders of 1 mm and 10 μm , respectively. Both spines and microbarbs have conical shapes, whose diameters gradually increase from the tip to the root of a wire. A water drop that is condensed, e.g., on the tip of

the spine or the microbarb can be driven to the root by a capillary force induced by this diameter gradient.⁶ Moreover, the fog-collection behavior of the dune grasses *Stipagrostis subulicola* has been explored.⁴ They use their leaves and roots to collect the fog in Namib Desert. Water drops are first condensed on leaves. When the drops become too large to be supported by the leaves, they fall to the roots, which spread over 20 m like a carpet. A similar approach is also used by *cotula fallax* plants to collect fog.⁵ In addition, spider silk is found to have capability of collecting fog as well.⁷ Because of a capillary force generated by the conical shape and different roughnesses of the silk surface, water drops can be guided to specific locations on the silk.

Several artificial fog collectors have been recently developed, which mimic the fog-collection mechanisms of beetles.^{8–11} In addition, under the inspiration of the cacti, conical-shaped copper wires¹² have also been employed to collect fog. It is expected that when branched wires are incorporated into such a wire to form a branched wire structure as in the case of cacti, water-collection efficiency will be increased because of the increase in the surface area of the corresponding structure. Accordingly, in this work, we desire to develop branched ZnO wire structures for water collection. As in the case of a cactus, all the wires in a branched ZnO wire structure will have conical shapes for guiding the movements of water drops, and their

Received: November 25, 2013

Accepted: February 5, 2014

Published: February 5, 2014

lengths will be comparable to or longer than the counterparts of the cactus.

ZnO wires have attracted much attention in the past decade because of their specific properties of piezoelectricity, semiconductivity and wide bandgaps. They have been employed as functional components of microelectronic,^{13,14} optoelectronic,^{15–17} microfluidic devices,¹⁸ power generators,^{19,20} and superhydrophobic surfaces.^{21,22} They have also been applied in various sensors, such as humidity,²³ gas,²⁴ chemical,²⁵ and biosensors.²⁶ The single ZnO wires reported by other researchers to date only have lengths up to 300 μm ,²⁷ implying that it is an obstacle to fabricate millimeter-long stem wires. Moreover, different from existing ZnO wires which normally have uniform cross-sections, ZnO wires in the proposed structures should have conical shapes, which presents a second obstacle in the corresponding synthesis. These two obstacles will be specially overcome in fabricating the desired structures.

2. WATER-COLLECTION TESTS ON A CACTUS, AND THEORETICAL BACKGROUND

Water-collection mechanism of a cactus has been reported previously.³ To have a better understanding about this mechanism, we also explore the cactus *Opuntia engelmannii* var. *lindheimeri* that can be found in our campus. It has surface structures similar to what was reported for the cactus *O. microdasys*.³ The cactus *Opuntia engelmannii* var. *lindheimeri* also has an array of clusters on its pad surface (Figure 1a1), and every cluster contains tens of branched wire structures (Figure 1a2, a3). Both spine and microbarbs in a branched wire structure have conical shapes with apex angles of about 8 and 18°, respectively (Figure 1a4–a6). The spine has a length ranging from 0.73 to 2.43 mm, and the diameter of its middle cross-section is about 80 μm . The microbarb has a length between 18 and 50 μm , and the diameter of its middle cross-section is about 11 μm .

At room temperature ($22\text{ }^{\circ}\text{C} \pm 1\text{ }^{\circ}\text{C}$), a humidifier (model: EE-5301, Crane USA Co.) was employed to generate a mist flow over a branched wire structure of the cactus *Opuntia engelmannii* var. *lindheimeri*, which implies that relative humidity was 100% in the tested area (Figure 2). The humidifier was turned on for 1 min to ensure that the flow rate was steady. Subsequently, a branched wire structure of the cactus was placed in the mist flow, followed by the recording of the water-collection process through an optical microscope. The flow was along the longitudinal direction of the branched wire structure. As shown in panels b and c in Figure 1 and illustrated in Figure 1d, a representative process that a cactus collects water is as follows. A small water drop first appears on the tip of a branched wire (Figure 1d1, c1), because the tips of the branched wires are directly exposed to the mist flow. There may also exist water drops on the sidewall of the branched wire. However, because this sidewall is not directly exposed to the flow, such drops may not be as large as the one on the tip. Accordingly, these drops are not found at the beginning of our test (see, for example, Figure 1c1). Similar phenomena have been previously observed in the case of *The President* lotus.²⁸ As indicated previously,⁶ the small drop then moves from the tip to the root along this branched wire (Figure 1c2). In such a manner, small water drops that are formed at the tips of the branched wires at different time instants continuously move to the roots (Figure 1d2, c3). After that, they merge to form a large drop (Figure 1d3). The large drops located on the roots of the branched wires then move to the root of the stem wire,

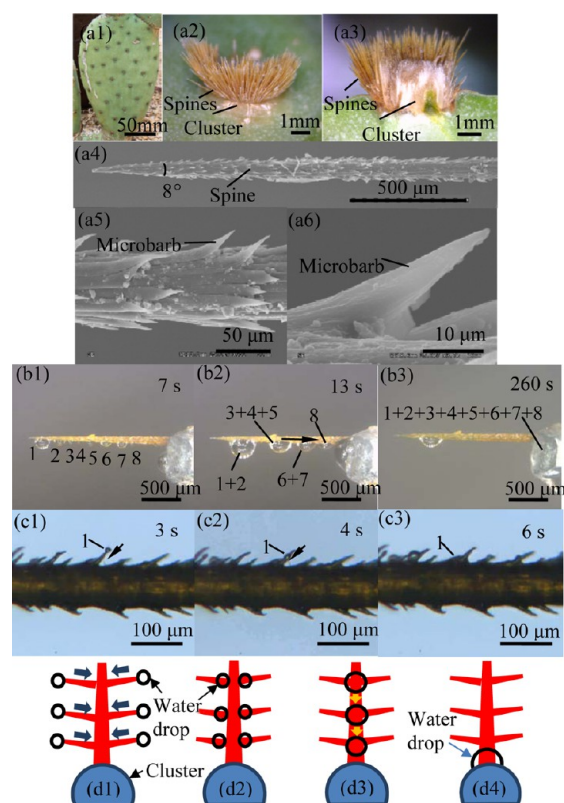


Figure 1. (a1) Pad of the cactus *Opuntia engelmannii* var. *lindheimeri*, whose surface is distributed with an array of clusters, (a2) side and (a3) cross-sectional views of a single cluster, which is covered by a bunch of spines. A branched wire structure, consisting of (a4) a 1.8-mm-long spine and (a5, a6) microbarbs on a cluster. a1–a3 are optical images, whereas a4–a6 are SEM ones. Water collection of a cactus through (b) a spine and (c) microbarbs. Illustration of a water-collection process of the cactus: (d1) small drops are formed on tips of branched wires, (d2) move down to the roots of these wires, and (d3) merge to form large drops, which (d4) subsequently move down to the root of the stem wire to form a larger drop. All drawings or pictures are side or top views, and numbers in b1–b3 and c1–c3 represent different water drops.

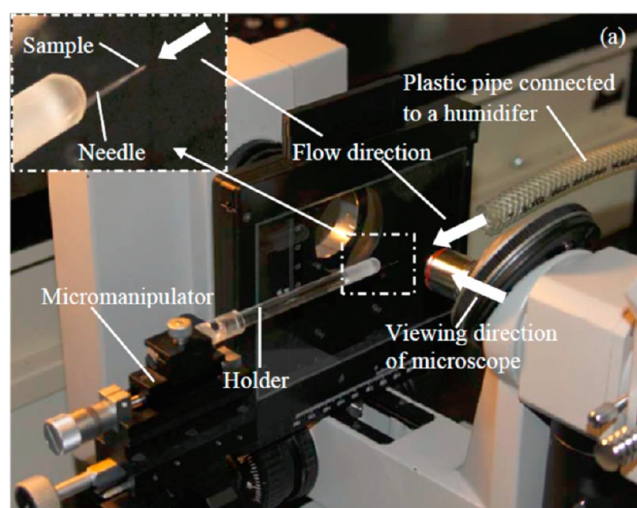


Figure 2. Experimental setup for water collection.

merging over there to form a much larger drop, which is subsequently collected by the underneath cluster (Figure 1d4,

b). Within 260 s, all the water drops that we specifically observed have moved to the root of the stem wire (Figure 1b3). Repetition of this process continuously provides water into the cluster. The same procedure is subsequently used in proposed branched wire structures to collect water.

A quasi-spherical liquid drop on a thin, conical wire suffers a capillary force, which has the following expression⁶

$$dP/dz = -\gamma\theta/(r + R_0)^2 \quad (1)$$

where P denotes Laplace pressure inside a liquid drop, z the position of the drop on the wire, dP/dz Laplace pressure gradient along the wire (also representation of the capillary force), γ surface tension of the liquid, θ the apex angle, r the mean radius of the wire at the place where the drop is located, and R_0 the mean radius of the drop. Three points can be observed from this equation. First, when θ is zero, i.e., a wire has uniform cross-section, the corresponding capillary force is zero. Accordingly, a liquid drop does not move on this wire. Thus, a conical shape is needed. Second, the capillary force increases with the decrease in the wire radius and the increase in the apex angle, implying that thin wires with large variations in cross sections are preferred in water collection. Third, the capillary force also increases with the decrease in the drop volume, which means that a small drop moves faster than a large drop on a conical wire. All three points have been validated in the above tests on the cacti (Figure 1b, c) as well as in the previously reported tests.³

3. FABRICATION

3.1. Fabrication Procedure. Branched ZnO nanowire structures have been recently synthesized using, for example, vapor-phase,^{29–32} solution-synthesis^{33,34} or their combinations.³⁵ Their large surface areas make them have potential applications in, for example, solar energy conversion.^{35,36} The concern here is how to make much larger branched structures.

There is a critical difference between the approaches of vapor phase and solution synthesis: the temperature used in a vapor-phase method normally ranges between 600 and 1000 °C,^{29–32} whereas the one adopted in solution synthesis method usually varies between 80 and 100 °C.^{33,34} Because of this large difference in growth temperature (accordingly, there is a large difference in growth energy), during the same time period, wires grown using the vapor-phase approach are much longer (the lengths of the longest wires were reported to be 300 μm)²⁷ than the counterparts grown using the solution synthesis (the longest wires had the lengths of 40 μm).³⁷ Thus, a vapor-phase approach is applied in our case to produce long stem and branched wires.

Vapor–solid (VS)^{29,30} and vapor–liquid–solid (VLS)^{31,32} are two commonly applied vapor-phase methods. The VS method is adopted here to grow wires, because we have rich experience with this approach. In the VS, the substrate is coated with a layer of ZnO. The Zn and O₂ atoms are directly adsorbed on the surface of this ZnO seed layer, forming nuclei. ZnO wires grow out vertically from the nuclei in c -axis orientation. In the VS method, the substrate is coated with a layer of ZnO. The Zn and O₂ atoms are directly adsorbed on the surface of this ZnO seed layer, forming nuclei. ZnO wires grow out vertically from the nuclei in c -axis orientation.

The synthesis of branched ZnO wire structures involves two basic steps (Figure 3). In the first step, stem wires are selectively grown on the ZnO film-covered sidewall of a Si

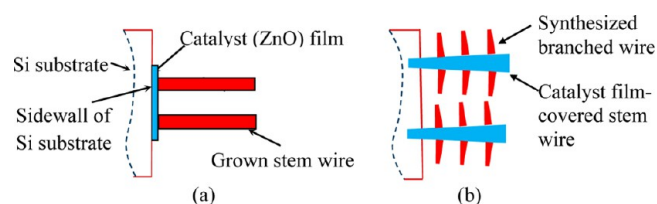


Figure 3. Procedure to fabricate branched ZnO wire structures (schematics): (a) Grow stem wires on the catalyst (ZnO) film located on the sidewall of a Si substrate, and (b) further synthesize branched wires on the catalyst film-covered sidewall of each stem wire.

substrate using a VS method^{29,30} (Figure 3a). In the second step, using the VS approach again, branched wires are synthesized on the ZnO film-covered sidewall of each stem wire, completing the fabrication of a branched structure (Figure 3b). Three types of experiments are conducted. The first type of experiment is to grow ZnO stem wires, which corresponds to the first fabrication step. The second type is to examine the possibility of synthesizing relatively long wires on the sidewall of a long wire, and the third is to grow branched wires on the stem wires, which corresponds to the second fabrication step.

3.2. Synthesis of Stem Wires. Figure 4a shows a setup used in the first type of experiments. It includes a horizontal tube furnace and a quartz boat. ZnO and graphite powders are mixed on the surface of the quartz boat, which is subsequently placed in the center of the furnace. A Si substrate is placed on the quartz boat. After the tube in the furnace is heated up from room temperature to 950 °C, Ar and O₂ gases are introduced into the reactor. Meanwhile, Zn vapor is continuously generated by carbothermal reduction of ZnO powder in the graphite crucible, following the chemical reaction: $\text{C(s)} + \text{ZnO(s)} \rightarrow \text{CO(g)} + \text{Zn(g)}$. The produced Zn vapor is brought over by the incoming gas flow to the Si substrate, and has reaction with O₂ over there to produce ZnO wires. After the high temperature is maintained for 20 h, Ar and O₂ systems are switched off and the furnace is cooled naturally to room temperature. The incoming Ar and O₂ flow have horizontal speeds of 85 and 2 sccm, respectively, whereas their vertical speeds are both zero.

The quartz boat consists of a horizontal plate and a movable vertical support. The horizontal plate has a small step on its back side. The substrate is put between this step and the vertical support. By moving the vertical support forward or backward along the horizontal plate, the substrate can be tilted at different angles. Consequently, the orientation of this substrate can be adjusted between 0 and 90° relative to the incoming gas flow.

Other researchers usually set the tilt angle to be 0° when growing ZnO structures.^{27,29–33,38} However, in the first type of experiments, we changed the tilt angle to be 30° (Figure 4a), resulting in a clear difference in the products generated on the edges and top surface of a Si substrate. An “edge effect” was found on the synthesized product. As shown in Figure 4b1, the lengths of ZnO wires were 484 μm on the top surface of the Si substrate, whereas ZnO wires grown on the edges of this substrate had the lengths of 4 to 5.5 mm, which are about 10 times longer than the ones on the top surface. The average diameters of the grown wires were 1 μm (Figure 4b2). The selected-area electron diffraction (SAED) pattern of a 4-mm-long wire (the inset of Figure 4b3), together with the top view of a representative ZnO wire (the inset of Figure 4b2), shows that the ZnO wire has a hexagonal wurtzite structure with the

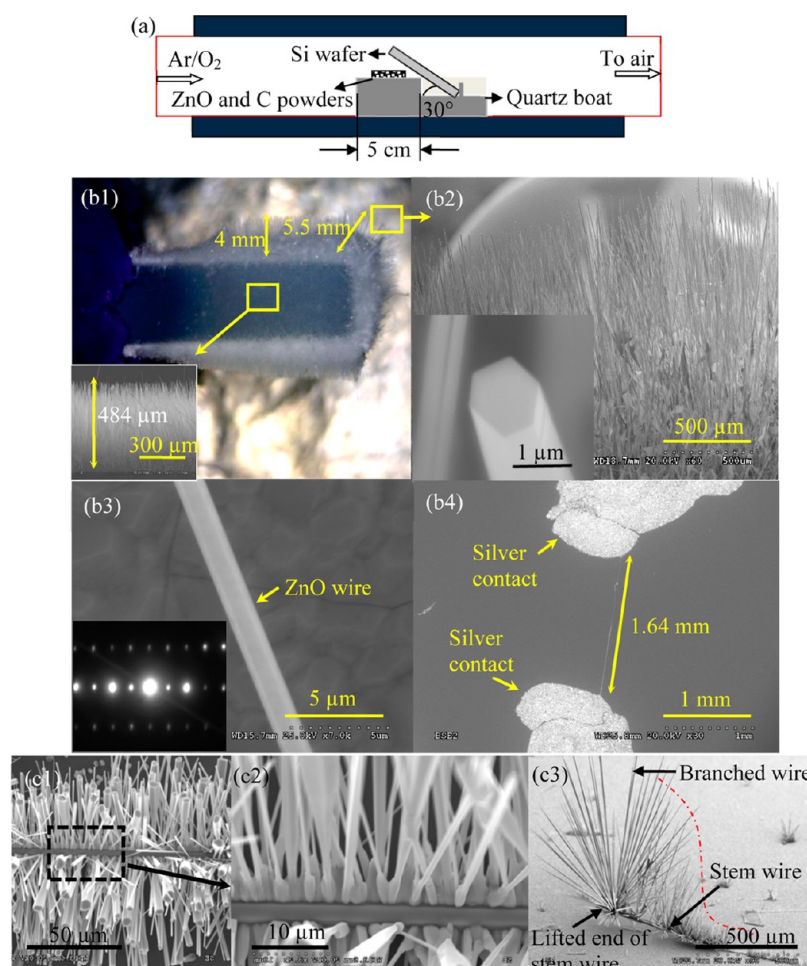


Figure 4. (a) Side view of a setup employed in the first two types of experiments to synthesize ZnO wires. (b1) Optical image of ZnO wires grown using this setup: wires with lengths of $484\ \mu\text{m}$ were grown on the top surface, whereas wires with lengths of 4 to 5.5 mm were synthesized on the side edges of a silicon substrate (inset: side view of the $484\text{-}\mu\text{m}$ -long wires); (b2) close-up (SEM) view of the 5.5-mm-long ZnO wires (inset: perspective view of the top of a ZnO wire, indicating that it has hexagonal cross sections); (b3) side (SEM) view of a ZnO wire (inset: the corresponding SAED pattern); and (b4) top (SEM) view of a 1.64-mm-long wire connected to two Ag pads at its ends. Branched wires generated on (c1) and (c2) a 4-mm-long flat wire, and on (c3) a partially lifted wire.

growth direction along the direction of $[0001]$ (i.e., c -axis). The first type of experiments indicates that, using our setup, it is feasible to generate mm-long stem wires on the sidewall of a Si substrate.

The “edge effect” is interpreted as follows. When a substrate experiences a gas flow, a relatively stagnant layer (i.e., a boundary layer) is formed on the surface of this substrate. The gaseous reactants have to diffuse through this boundary layer in order to reach the surface of the substrate to form the wires, and the concentrations of the gaseous reactants on this surface increase with the decrease in the thickness of this boundary layer.³⁹ According to Prandtl’s boundary-layer theory,⁴⁰ the boundary layer at the substrate edge is much thinner than that in the middle of the substrate, resulting in higher gas concentrations at the edges. In other words, during the same time period, the substrate edge experiences more gaseous reactants than the middle of the substrate. Thus, the ZnO wires grown on the edges were much longer than those at the center of the substrate in the first type of experiments.

3.3. Growth of Branched Wires. Another experimental setup was adopted in the second and third types of experiments. It is similar to the one used in the first type of experiments, except for two critical differences (Figures 4a and

5a): (i) a flowerpot-like crucible, which had a top opening with the diameter of 2 cm, was applied to contain ZnO and graphite powders; and (ii) the Si substrate was directly placed on the top opening of the crucible. Both changes were made to ensure that the ZnO wires were directly exposed in the incoming flow of Zn vapors.

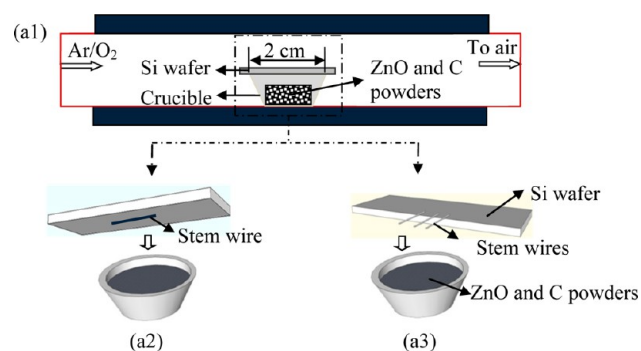


Figure 5. (a1) Side view of the setup for (a2) the second and (a3) third types of experiments.

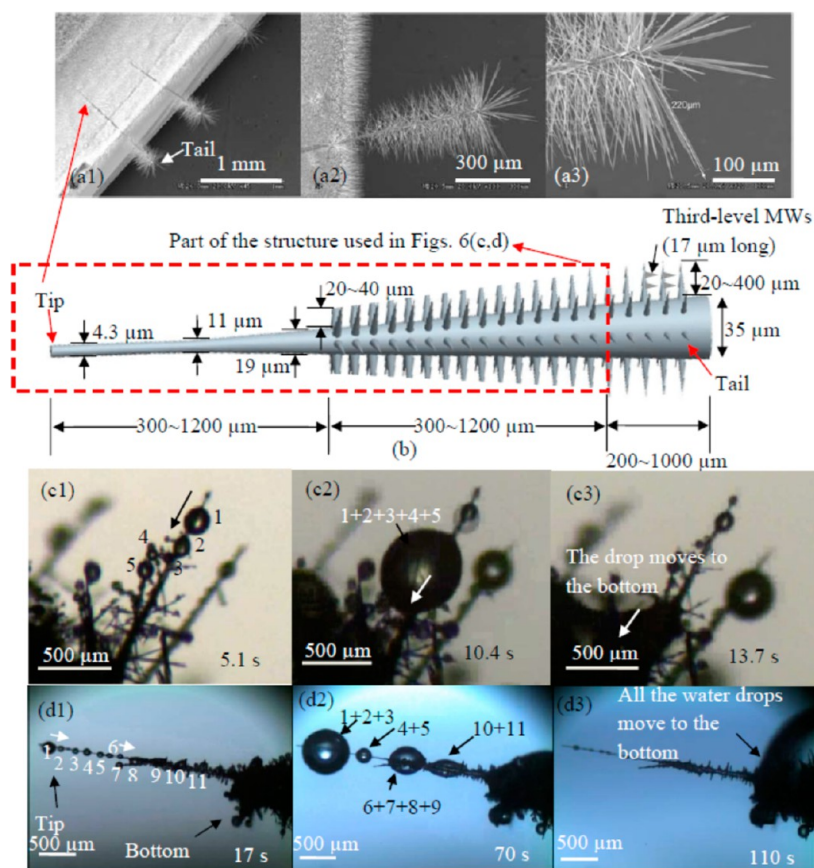


Figure 6. Synthesized branched wire structures: (a1) perspective view of three structures, (a2) close-up view of one of three structures, and (a3) magnified view of its tail portion. (b) Schematic of a synthesized structure. (c, d) Transportation and mержence of water drops on a synthesized branched wire structure: (c1) due to condensation of vapors, water drops appear on a branched wire, (c2) some drops merge into a large water drop in the middle of the branched wire, and (c3) the large drop further moves to the root of this wire. Transportation and mержence of large drops on the stem wire: (d1) water drops appear on the stem wire, (d2) these drops merge together to form several large drops, and (d3) the large drops move to the root of this stem wire.

In the second type of experiments, we examined whether long branched wires could be grown on the sidewall of a single wire to form a branched structure. The stem wires that were synthesized on the substrate edges in the first type of experiments were first manually placed on the center of a Si wafer (Figure 5a2). The ZnO wires have an inherent charge. Accordingly, after a ZnO stem wire was put on the Si wafer, the electrostatic interactions⁴¹ between them directly fixed the wire on the Si wafer. This Si wafer was subsequently flipped down on the crucible. The second type of experiments includes two tests. In the first test, branched wires with lengths of about 30 μm were synthesized on the sidewalls of a 4-mm-long flat wire (Figure 4c1, c2). Furthermore, in the second test, one end of a flat wire was lifted up before the growth of branched wires. As shown in Figure 4c3, branched wires with lengths as long as 800 μm were grown on the lifted end of this wire (which was about 27 times as long as the ones generated in the previous test), and the lengths of the branched wires decreased from the lifted end toward the middle point of the flat wire, indicating that the “edge effect” can also be used to generate long branched wires. On the basis of the understanding gained from the first two types of experiments, branched wires were further grown on the stem wires in the third type of experiments. Part of a stem wire was put on the top surface of a Si substrate, whereas the remaining portion remained open to ensure that

this portion was directly exposed to both Zn vapors and O_2 gases (Figure 5a3).

Figure 6a gives three representative branched wire structures synthesized out of the third type of experiments. Both stem and branch have conical shapes with apex angles of about 2 and 15°, respectively. The stem wire has a length ranging from 0.8 to 3.4 mm, and the diameter of its middle cross-section is about 25 μm . A branched wire has a length in the range of 20 to 400 μm , and the diameter of its middle cross-section is around 10 μm . These parameters are approximately in the same order as those of a branched wire structure on a cactus surface, whereas some branched wires are 7 times longer than their cactus counterparts (Figure 1a6).

All the wires in the synthesized structures have conical shapes. Because of “edge effect”, the reactant concentration at a point of the stem wire gradually increases with the increase in the distance between this point and the substrate sidewall, resulting in two consequences. First, as observed in the second test of the second type of experiments, branched wires grown toward the open end of a suspended wire are longer than those close to the fixed end of this wire (Figure 4c3). Second, the suspended wire gradually became thicker from the fixed end to the open one, forming a conical shape (Figure 6b). On the other hand, the thickness of this wire increases at a lower rate than the length of a branched wire, because the sidewall growth of the wire is not along the preferred direction.

The formation of a conical branched wire is caused by two factors. First, a new portion of a wire is formed on the top surface of an existing part, and the cross-section of the new portion cannot be larger than that of the existing part. Second, Zn vapor concentration gradually decreases during the process of fabricating the branched wires, resulting in the decrease in chemical reaction rate. Accordingly, as previously reported,⁴² the new portions of branched wires have smaller cross sections than the existing parts, forming conical shapes. The gradual reduction of Zn concentration is interpreted as follows. As observed from panels a1 and a3 in Figure 5, O₂ gas has chemical reaction with Zn vapor at the top opening of the crucible to form branched wires. In addition, this reaction also occurs inside the crucible, which creates a thin ZnO film on top of the source materials (the film can be visibly seen after the fabrication is finished). This film gradually increases its area during the synthesis process, covering more source materials. Accordingly, the amount of Zn vapor that comes from the uncovered portion of the source material is gradually decreased, resulting in a lower Zn concentration around branched wires. However, this is not the case during the process of synthesizing stem wires in the first fabrication step. Because of the “edge effect” and the driving effect of Ar flow, a less amount of O₂ stays on the surface of source materials (Figure 4a). Consequently, the created thin ZnO film just covers a small portion of the source materials. In addition, the surface area of the source materials is about 4.5 times as large as that in the process of fabricating branched wires. Thus, enough Zn vapor has been produced during the process of generating stem wires, making these wires have relatively uniform cross-sections.

4. WATER-COLLECTION TESTS ON ARTIFICIAL STRUCTURES

4.1. Water-Collection Process. The synthesized branched wire structures were subsequently examined for their capability

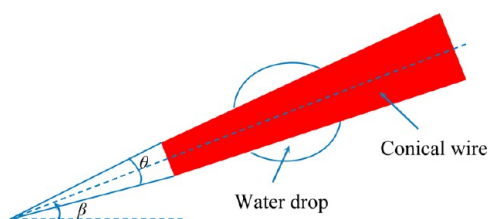


Figure 7. Geometric model of a water drop on a conical wire.

of collecting water using a setup the same as the one shown in Figure 2. As marked in Figure 6b, the major part of a structure was used in such a test. After it was flipped, the corresponding tail portion was manually fixed on the tip of a needle using superglue (Henkel Co., CT, USA), whereas the rest part remained open to incoming water vapors. Panels c and d in Figure 6 give some testing results. The movements of condensed water vapors on both branched (Figure 6c) and stem (Figure 6d) wires are similar to what was observed on a cactus branched wire structure (Figure 1b, c), and match what was illustrated in Figure 1d. Within 110 s, all the drops that were specifically observed moved to the root of the tested structure (Figure 6d3).

We noted that a water drop could still be collected even if a branched wire was oriented along the vertical direction with its tip located at the lower position, implying that all the wires in a structure have the capability of collecting water no matter what

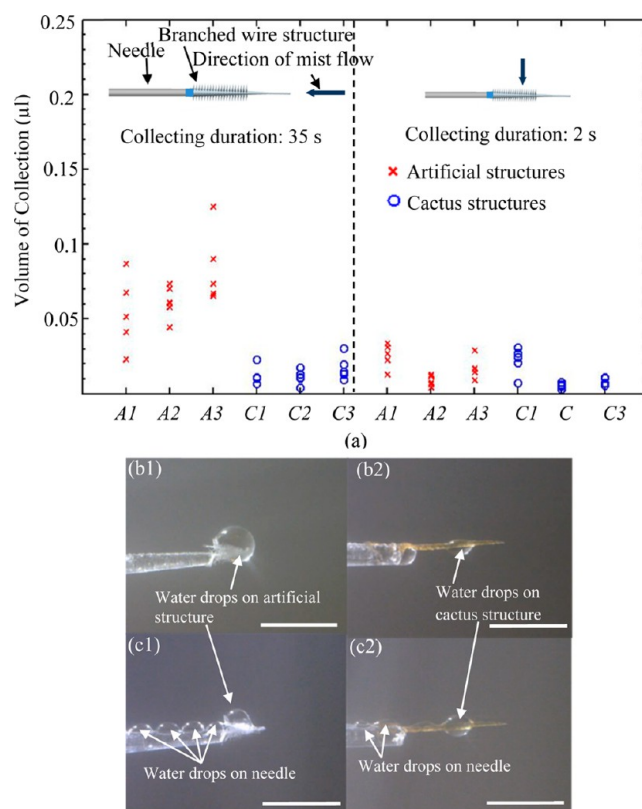


Figure 8. (a) Comparison of collected water between artificial and cactus branched wire structures. A1–A3 and C1–C3 denote artificial and cactus structures, respectively. Water drops collected by (b1) artificial (A1) and (b2) cactus (C1) structures in the first group of tests at the time instant of 35 s. Water drops collected by (c1) artificial (A1) and (c2) cactus (C1) structures in the second group of tests at 2 s. The scale bars represent 1 mm.

their orientations are. This phenomenon is interpreted using a theoretical result derived previously.⁶ Let β denote the maximum tilt angle of the wire that water drop moves upward along the wire (Figure 7). Then, $-90^\circ \leq \beta \leq 90^\circ$ and we have⁶

$$\sin \beta = \frac{\theta l^2}{(r + \sqrt[3]{3V/4\pi})^2} \quad (2)$$

where l represents capillary length of water and equals 2.7 mm, and V is the drop volume. Three points can be observed from this equation. First, for a given water drop, β increases with the increase in θ and decrease in r . Second, if a wire has uniform cross sections, which corresponds to the case that $\theta = 0^\circ$, then $\beta = 0^\circ$. This result implies that water could not move along the wire no matter how this wire is oriented, and that the wire should have varied cross sections to make a water drop move. Third, when $\beta = 90^\circ$, which is the maximum tilt angle that a wire could have, in order to make water drops move upward, by eq 2, the volume of a water drop should meet the following relation

$$V \leq \frac{4\pi}{3} (l\sqrt{\theta} - r)^3 \quad (3)$$

According to the values of θ (about 15°) and r (around $5 \mu\text{m}$ on average) for a branched wire, eq 3 indicates that if the volume of a water drop is not larger than 0.01 mL, then it can move upward along a branched wire. On the basis of the values of θ (about 2°) and r (around $12.5 \mu\text{m}$ on average) for a stem

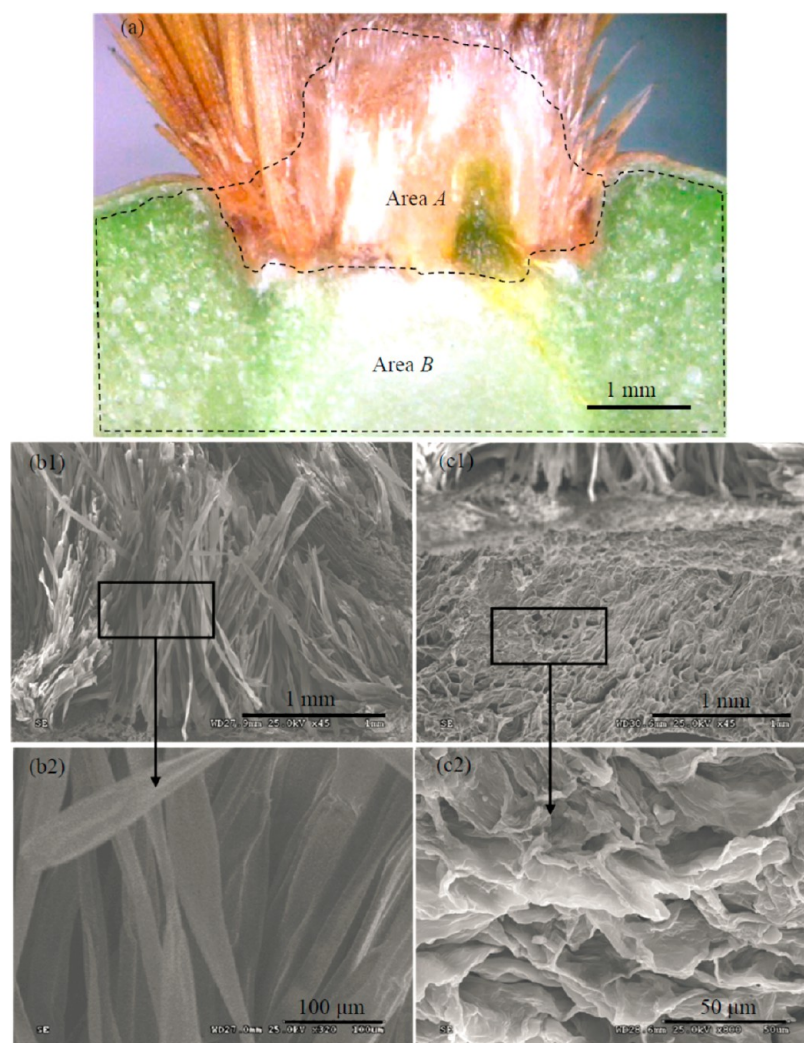


Figure 9. (a) Cross-sectional (digital) image of a cluster on the cactus *Opuntia engelmannii* var. *lindheimeri*. Close-up (SEM) views of areas (b) A and (c) B.

wire, eq 3 shows that, if the drop volume is not larger than 0.0005 mL, then it can move upward along the stem wire even if $\beta = 90^\circ$. On the other hand, according to our tests, a water drop has already moved upward to the root along a vertically oriented branched wire when the drop volume is far below 0.0005 mL. As observed from eq 1, small water drops are easier to move than larger drops, because they suffer larger capillary forces. Hence, both stem and branched wires in the synthesized structure are capable of collecting water no matter how they are oriented.

4.2. Comparison of the Water Collection between Artificial and Cactus Structures. Two groups of tests were done to compare water-collection efficiency of three artificial structures with another three cactus spines when the incoming mist flows had different directions (Figure 8a). The mist flow direction was parallel to the longitudinal direction of a branched wire structure in the first group of tests, while it was perpendicular in the second group. In either group of tests, the artificial and cactus structures were each tested for five times. The stem wires in the three artificial structures, which are labeled as A1, A2, and A3 in Figure 8a, have lengths of 0.5, 0.64, and 1.12 mm, respectively. The three cactus structures are called C1, C2, and C3, which have lengths of 1.32, 0.77, and 1.53 mm, separately. It took an artificial structure a shorter time

than a cactus one to collect a large drop, which covered the whole artificial structure (Figure 8b1, c1). After this had occurred, the continuous collection of water relied on the adsorption of water vapors to the large drop, instead of the transportation of condensed drops through the wires. Accordingly, the time duration that we chose to compare water collection in a group of tests was the shortest period that it took collected water to cover an artificial structure among all the tests in this group. In the second group of tests, the flow direction was approximately perpendicular to the longitudinal direction of the branched wires that were located on the top half sidewall of the stem wire, whereas smaller amounts of branched wires were directly exposed to the mist flow in the first group of tests. Consequently, the collecting duration of interest in the second group of tests was found to be 2 s (Figure 8c1). It was much shorter than the one in the first group tests, which was 35 s (Figure 8b1).

In the first group of tests, the amount of water collected by the artificial structure had a volume varying from 0.023 to 0.125 μL , which was calculated based on the measured diameter of a collected drop, and such a volume ranged from 0.004 to 0.03 μL in the case of the cactus structure. The average volumes collected by the artificial and cactus structures were 0.067 and 0.013 μL , respectively. This 5-time difference indicates that the

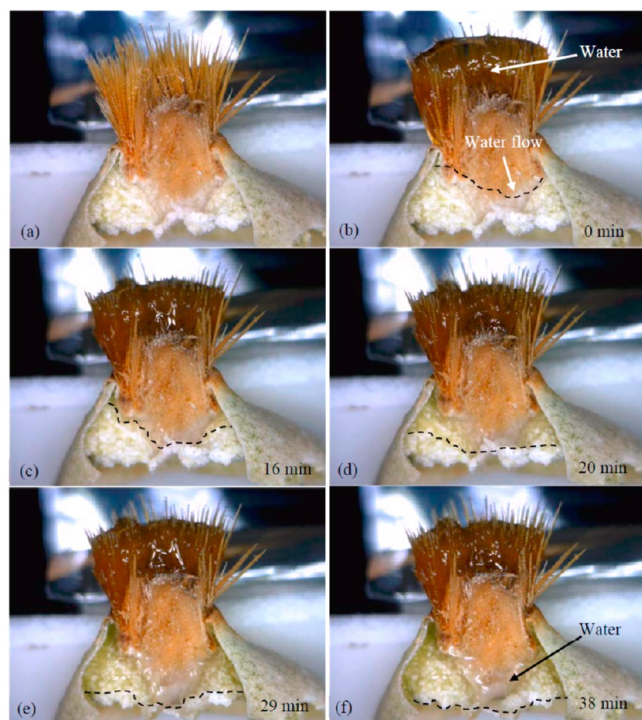


Figure 10. In situ observation of the process that water was absorbed into a dried cactus cluster from its surface: (a) before and (b) after a large water drop was put on the cluster, and (c–f) water slowly moved inside the cluster. The dashed lines in b–f represent the fronts of water flow.

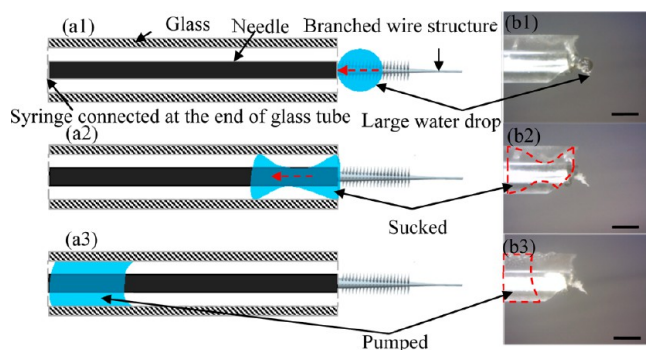


Figure 11. (a) Schematic and (b) experimental results of water collection process for one cycle. (a1, b1) A large drop is collected at the root of an artificial branched wire structure. (a2, b2) This large drop is sucked into glass tube by a capillary force. (a3, b3) The sucked water is pumped by the syringe from right to left, completing this cycle of collection. The scale bars represent 1 mm.

artificial structure, in comparison with the cactus one, is more efficient in collecting water due to larger surface areas of its branched wires (some branched wires are 8.0 times as long as those of a cactus, and they are also more densely distributed on the stem wire). The comparison shows the importance of having ultralong stem and long branched wires, which increase the surface areas of the structure for adsorbing more water vapors.

In the second group of tests, the volume of water collected by the artificial structure varied from 0.004 to 0.034 μL , whereas it ranged from 0.003 to 0.031 μL in the case of the cactus structure. The average volume collected by the artificial structure was 0.017 μL . It was about 1.4 times as large as that

harvested by the cactus one, which was 0.012 μL . In this group of tests, water vapors were condensed on the whole surface of a structure, and they also quickly penetrated into the gaps between branched wires. Hence, water was not mainly collected by the movement of the drops on the wires. This point can also be observed from panels c1 and c2 in Figure 8. Water drops were formed on needle surfaces as well, and had comparable sizes with those formed on the artificial or cactus structures, even if these surfaces were not covered by branched wires. In contrast, such phenomena were not observed in the first group of tests (Figure 8b1, b2), indicating that branched wires play an important role in collecting water when a structure is not directly exposed to the mist flow.

4.3. Continuous Collection of Water by an Artificial Structure. To explore the possibility of collecting water continuously by the as-grown branched wire structures, we first examined that mechanism that a cactus employed to absorb collected water drops from its branched structures into their underneath cluster. The test was on a dried cluster, whose cross-sectional view is given in Figure 9. The inner structure of the cluster, which is marked as “Area A” in Figure 9a, is an array of hairlike trichomes.⁴³ These dried trichomes have relatively flat shapes (Figure 9b2), probably due to loss of water. They have an average width of about 50 μm , and their lengths range from 0.3 to 3 mm. Underneath the cluster is thin-walled parenchyma,⁴⁴ which is labeled as “Area B” in Figure 9a. Parenchyma is a water-storing tissue, and has a porous structure (Figure 9c). As a drop of water was manually placed on a dried cluster, through capillary action, water gradually flowed into a large portion of the parenchyma via the gaps between the trichomes within 38 min (Figure 10). As indicated in ref 45, the trichomes served as pathways during this water-absorption process. It is expected that, when the cactus is alive, the corresponding rate of water absorption may be much higher, because a water pressure difference can be created between the parenchyma and the cluster surface. This difference is induced by the loss of water inside the cactus, which may be caused by either (i) the transpiration⁴⁵ from the cactus surface, or (ii) the photosynthesis inside the cactus.⁴⁶

On the basis of the observed process of water absorption inside a dried cactus cluster, we then made three changes to the previous experimental setup (Figure 2) to continuously collect water through an artificial structure (Figure 11a): (i) a needle was located inside a glass tube with an inner diameter of 1.4 mm, (ii) a branched wire structure was positioned at the end of the glass tube that faced incoming mist flow, and (iii) a syringe was connected to the other end of the glass tube. The glass tube was applied to play the roles of both trichomes and parenchyma: guide a water flow, and store water. The syringe was used to create a pressure gradient for driving the collected water drops into the glass tube.

The mist flow direction was parallel to the longitudinal direction of a branched wire structure. A typical cycle of water collection includes three steps. First, water was first collected by the branched wires, and it then moved to the root of the structure (Figures 11a1, b1). Second, the collected water was sucked into the glass tube due to a capillary force, which was caused by the curvature difference between the portion of the water drop outside and inside the glass tube (Figures 11a2, b2). Third, the syringe was employed to pump the sucked water from right to left side of the glass tube (Figures 11a3, b3). Water was continuously collected for 30 min. Twenty cycles

occurred during this period, the time for each cycle varied from 60 to 100 s, and in total about 6 μL of water was collected.

5. SUMMARY AND CONCLUSIONS

In this work, motivated by the water-collection approach of a cactus, we have developed an artificial branched wire structure to harvest water from fog and dew. An edge effect is employed to synthesize such a structure. As in the case of the cactus, all these wires in this structure have conical shapes, yielding a capillary force to drive a water drop to move from the tip of a wire to the root. On the other hand, due to relatively larger surface areas of the branched wires in the artificial structure, this structure collected more water in comparison with the cactus structure. In addition, it is also found that the amount of water collected is related to the direction of the incoming vapor flow. Finally, we have demonstrated that, with the aid of a syringe, large drops located at the root of a branched wire structure can be pumped into a glass tube, making this structure capable of continuously collecting water.

AUTHOR INFORMATION

Corresponding Author

*E-mail: chengluo@uta.edu.

Author Contributions

†Authors X.H. and M.X. contributed equally.

Notes

The authors declare no competing financial interest.

ACKNOWLEDGMENTS

This work was supported in part through NSF-CMMI-1030659 grant.

REFERENCES

- (1) Middleton, N. *Deserts: A Very Short Introduction*; Oxford University Press: New York, 2009; pp 4, 16, 19.
- (2) Parker, A. R.; Lawrence, C. R. Water capture by a desert beetle. *Nature* **2001**, *414*, 33–34.
- (3) Ju, J.; Bai, H.; Zheng, Y.; Zhao, T.; Fang, R.; Jiang, L. A multi-structural and multi-functional integrated fog collection system in cactus. *Nat. Commun.* **2012**, *3*, 1247.
- (4) Ebner, M.; Miranda, T.; Roth-Nebelsick, A. Efficient fog harvesting by *Stipagrostis sabulicola* (Namib dune bushman grass). *J. Arid Environ.* **2011**, *75*, 524–531.
- (5) Andrews, H.; Eccles, E.; Schofield, W.; Badyal, J. Three-dimensional hierarchical structures for fog harvesting. *Langmuir* **2011**, *27*, 3798–3802.
- (6) Lorenceau, É.; Quéré, D. Drops on a conical wire. *J. Fluid Mech.* **2004**, *510*, 29–45.
- (7) Zheng, Y.; Bai, H.; Huang, Z.; Tian, X.; Nie, F.-Q.; Zhao, Y.; Zhai, J.; Jiang, L. Directional water collection on wetted spider silk. *Nature* **2010**, *463*, 640–643.
- (8) Zhai, L.; Berg, M. C.; Cebeci, F. C.; Kim, Y.; Milwid, J. M.; Rubner, M. F.; Cohen, R. E. Patterned superhydrophobic surfaces: toward a synthetic mimic of the Namib Desert beetle. *Nano Lett.* **2006**, *6*, 1213–1217.
- (9) Garrod, R.; Harris, L.; Schofield, W.; McGettrick, J.; Ward, L.; Teare, D.; Badyal, J. Mimicking a stenocara beetle's back for microcondensation using plasmachemical patterned superhydrophobic-superhydrophilic surfaces. *Langmuir* **2007**, *23*, 689–693.
- (10) Dorrer, C.; Riihe, J. r. Mimicking the Stenocara Beetle Dewetting of Drops from a Patterned Superhydrophobic Surface. *Langmuir* **2008**, *24*, 6154–6158.
- (11) Thickett, S. C.; Neto, C.; Harris, A. T. Biomimetic surface coatings for atmospheric water capture prepared by dewetting of polymer films. *Adv. Mater.* **2011**, *23*, 3718–3722.

(12) Ju, J.; Xiao, K.; Yao, X.; Bai, H.; Jiang, L. Bioinspired Conical Copper Wire with Gradient Wettability for Continuous and Efficient Fog Collection. *Adv. Mater.* **2013**, *25*, 5937–5942.

(13) Park, W.; Yi, G.-C.; Kim, J.-W.; Park, S.-M. Schottky nanocontacts on ZnO nanorod arrays. *Appl. Phys. Lett.* **2003**, *82*, 4358–4360.

(14) Park, W. I.; Kim, J. S.; Yi, G.-C.; Bae, M.; Lee, H.-J. Fabrication and electrical characteristics of high-performance ZnO nanorod field-effect transistors. *Appl. Phys. Lett.* **2004**, *85*, 5052–5054.

(15) Kind, H.; Yan, H.; Messer, B.; Law, M.; Yang, P. Nanowire ultraviolet photodetectors and optical switches. *Adv. Mater.* **2002**, *14*, 158–160.

(16) Wang, X.; Summers, C. J.; Wang, Z. L. Large-scale hexagonal-patterned growth of aligned ZnO nanorods for nano-optoelectronics and nanosensor arrays. *Nano Lett.* **2004**, *4*, 423–426.

(17) Vispute, R.; Talyansky, V.; Choo-pun, S.; Sharma, R.; Venkatesan, T.; He, M.; Tang, X.; Halpern, J.; Spencer, M.; Li, Y. Heteroepitaxy of ZnO on GaN and its implications for fabrication of hybrid optoelectronic devices. *Appl. Phys. Lett.* **1998**, *73*, 348–350.

(18) Feng, X.; Feng, L.; Jin, M.; Zhai, J.; Jiang, L.; Zhu, D. Reversible super-hydrophobicity to super-hydrophilicity transition of aligned ZnO nanorod films. *J. Am. Chem. Soc.* **2004**, *126*, 62–63.

(19) Wang, Z. L.; Song, J. Piezoelectric nanogenerators based on zinc oxide nanowire arrays. *Science* **2006**, *312*, 242–246.

(20) Wang, X.; Song, J.; Liu, J.; Wang, Z. L. Direct-current nanogenerator driven by ultrasonic waves. *Science* **2007**, *316*, 102–105.

(21) Luo, C.; Xiang, M.; Heng, X. A stable intermediate wetting state after a water drop contacts the bottom of a microchannel or is placed on a single corner. *Langmuir* **2012**, *28*, 9554–9561.

(22) Luo, C.; Xiang, M. Angle inequality for judging the transition from Cassie–Baxter to Wenzel states when a water drop contacts bottoms of grooves between micropillars. *Langmuir* **2012**, *28*, 13636–13642.

(23) Zhang, Y.; Yu, K.; Jiang, D.; Zhu, Z.; Geng, H.; Luo, L. Zinc oxide nanorod and nanowire for humidity sensor. *Appl. Surf. Sci.* **2005**, *242*, 212–217.

(24) Fan, Z.; Wang, D.; Chang, P.-C.; Tseng, W.-Y.; Lu, J. G. ZnO nanowire field-effect transistor and oxygen sensing property. *Appl. Phys. Lett.* **2004**, *85*, 5923–5925.

(25) Fan, Z.; Lu, J. G. Gate-refreshable nanowire chemical sensors. *Appl. Phys. Lett.* **2005**, *86*, 123510–123510–3.

(26) Liu, T.-Y.; Liao, H.-C.; Lin, C.-C.; Hu, S.-H.; Chen, S.-Y. Biofunctional ZnO nanorod arrays grown on flexible substrates. *Langmuir* **2006**, *22*, 5804–5809.

(27) Wen, L.; Wong, K. M.; Fang, Y.; Wu, M.; Lei, Y. Fabrication and characterization of well-aligned, high density ZnO nanowire arrays and their realizations in Schottky device applications using a two-step approach. *J. Mater. Chem.* **2011**, *21*, 7090–7097.

(28) Xiang, M.; Wilhelm, A.; Luo, C. Existence and role of large micropillars on the leaf surfaces of the president lotus. *Langmuir* **2013**, *29*, 7715–7725.

(29) Conley, J., Jr.; Stecker, L.; Ono, Y. Directed assembly of ZnO nanowires on a Si substrate without a metal catalyst using a patterned ZnO seed layer. *Nanotechnology* **2005**, *16*, 292–296.

(30) Chakraborty, A.; Liu, X.; Wang, H.; Luo, C. Generation of ZnO nanowires with varied densities and lengths by tilting a substrate. *Microsyst. Technol.* **2012**, *18*, 1497–1506.

(31) Dalal, S.; Baptista, D.; Teo, K.; Lacerda, R.; Jefferson, D.; Milne, W. Controllable growth of vertically aligned zinc oxide nanowires using vapour deposition. *Nanotechnology* **2006**, *17*, 4811–4818.

(32) Huang, M. H.; Wu, Y.; Feick, H.; Tran, N.; Weber, E.; Yang, P. Catalytic growth of zinc oxide nanowires by vapor transport. *Adv. Mater.* **2001**, *13*, 113–116.

(33) Greene, L. E.; Law, M.; Tan, D. H.; Montano, M.; Goldberger, J.; Somorjai, G.; Yang, P. General route to vertical ZnO nanowire arrays using textured ZnO seeds. *Nano Lett.* **2005**, *5*, 1231–1236.

(34) Hsu, J. W.; Tian, Z. R.; Simmons, N. C.; Matzke, C. M.; Voigt, J. A.; Liu, J. Directed spatial organization of zinc oxide nanorods. *Nano Lett.* **2005**, *5*, 83–86.

- (35) Cheng, C.; Fan, H. J. Branched nanowires: Synthesis and energy applications. *Nano Today* **2012**, *7*, 327–343.
- (36) Bierman, M. J.; Jin, S. Potential applications of hierarchical branching nanowires in solar energy conversion. *Energy Environ. Sci.* **2009**, *2*, 1050–1059.
- (37) Qiu, J.; Li, X.; Zhuge, F.; Gan, X.; Gao, X.; He, W.; Park, S.-J.; Kim, H.-K.; Hwang, Y.-H. Solution-derived 40 μm vertically aligned ZnO nanowire arrays as photoelectrodes in dye-sensitized solar cells. *Nanotechnology* **2010**, *21*, 195602–195610.
- (38) Fan, H.; Fleischer, F.; Lee, W.; Nielsch, K.; Scholz, R.; Zacharias, M.; Gösele, U.; Dadgar, A.; Krost, A. Patterned growth of aligned ZnO nanowire arrays on sapphire and GaN layers. *Superlattices Microstruct.* **2004**, *36*, 95–105.
- (39) Sze, S. *VLSI Technology*, 2nd ed.; McGraw-Hill: New York, 1988.
- (40) Schlichting, H.; Gersten, K. *Boundary-Layer Theory*; Springer: Berlin, 2000.
- (41) Wang, M. C.; Gates, B. D. Directed assembly of nanowires. *Mater. Today* **2009**, *12*, 34–43.
- (42) Chang, P.-C.; Fan, Z.; Wang, D.; Tseng, W.-Y.; Chiou, W.-A.; Hong, J.; Lu, J. G. ZnO nanowires synthesized by vapor trapping CVD method. *Chem. Mater.* **2004**, *16*, 5133–5137.
- (43) Nobel, P. S., Ed.; *Cacti: Biology and Uses*; University of California Press: Berkeley and Los Angeles, CA, 2002; pp 23–27.
- (44) Slatyer, R. O. Absorption of water by plants. *Bot. Rev.* **1960**, *26*, 331–392.
- (45) Franke, W. Mechanisms of foliar penetration of solutions. *Annu. Rev. Plant Physiol.* **1967**, *18*, 281–300.
- (46) Govindjee, Ed.; *Photosynthesis V2: Development, Carbon Metabolism, and Plant Productivity*; Academic Press: New York, 1982.